

## Electronic Spectra of Two Polymorphs of (5-Dimethylamino-2,4-pentadienylidene)dimethylammonium Perchlorate

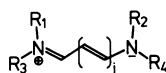
Norimichi SANO and Jiro TANAKA\*

Department of Chemistry, Faculty of Science, Nagoya University, Chikusa-ku, Nagoya 464

(Received October 28, 1985)

Reflection spectra were measured on two polymorphs of (5-dimethylamino-2,4-pentadienylidene)dimethylammonium perchlorate in order to determine the origin of the J band. One polymorph exhibited two bands with different polarization characteristics; one of them is explained by the molecular-exciton (MX) band of a  $\pi\pi^*$  transition character and the other is an intermolecular charge-resonance (CR) band, the polarization being along the direction connecting the nitrogen atoms of the adjacent molecules. The other polymorph exhibited a quasi-metallic reflection due to the overlapping of the CR and MX bands.

Cyanine dyes have a characteristic structure with an odd polymethine chain and two terminal nitrogen



atoms. It has been well known that the aggregate of the cyanine dye exhibits peculiar spectral characteristics in the visible region. Especially, the aggregation behavior and the spectral sensitization of photographic silver halide emulsions have been investigated.<sup>1–3)</sup>

From investigations of the spectra of some aggregates and those of crystals of cyanine dyes,<sup>4–6)</sup> it has been shown that a J band appeared in the crystals when the molecular overlap was significant in laterally shifted dye stacks. In such a condition, the charge-resonance (CR) configuration strongly interacted with the molecular-exciton (MX) configuration, where the interaction was assisted by a strong  $\pi$ -electron overlap. In contrast with the case of the crystals of electron donor-acceptor complexes, the intermolecular CR absorption band of pure molecular crystals have eluded direct observation for years, especially that of cyanine dyes, although electric field modulated spectra indicated the existence of intermolecular CR transition in 9,10-dichloroanthracene,<sup>7)</sup> for which the anomalous absorption polarization had been reported.<sup>8)</sup> The CR bands of anthracene,<sup>9)</sup> naphthalene and pentacene<sup>10)</sup> were also recently found.

In this paper, the reflection spectra and Kramers-Kronig (K-K) absorption spectra are presented on two polymorphs with space groups *Cc* (the yellow form)<sup>11)</sup> and *P2<sub>1</sub>/a* (the orange form),<sup>12)</sup> of (5-dimethylamino-2,4-pentadienylidene)dimethylammonium perchlorate (5-DMP, abbreviated to BDP in the literature).

Anex and Simpson<sup>13)</sup> reported a quasi-metallic reflectivity in the spectra of the yellow form, and its origin has been investigated theoretically by Philpott<sup>14)</sup> and Rimbey.<sup>15)</sup> On the other hand, Dähne and his coworkers<sup>16)</sup> have found the existence of an orange-colored crystal having the same constituent, and have

noticed a difference in the reflection spectra. Although Sieber et al. had reported the molecular and crystal structures of the orange form,<sup>17)</sup> a more precise X-ray analysis was performed by our group,<sup>12)</sup> and the molecular geometry with a bond-alternated character on the conjugated system and the charge-density distribution were determined.

In this paper, we present evidence of an intermolecular CR band between cation molecules in crystals of the orange form. Investigations regarding two modifications of a crystal of 5-DMP and a comparison with the previous study for 3-DMP ((3-dimethylamino-2-propenylidene)dimethylammonium perchlorate)<sup>18)</sup> are very illuminating for an assignment of the electronic transitions of the J-type band.

### Experimental

**Materials.** 5-DMP was synthesized by the method of Malhotra and Whiting.<sup>19)</sup> The product was purified with active charcoal and recrystallized several times from ethanol. Single crystals of the orange form were grown from methanol and those of the yellow form from ethanol. These were used for reflection measurements. Crystalline forms and faces were confirmed by taking X-ray photographs using the Weissenberg camera.<sup>11,12,17)</sup>

**Crystal Structures.** **The Orange Form:**<sup>12,17)</sup> Crystals of the orange form were prismatic (Fig. 1(a)) and were elongated along the *c* axis, showing the {100}, {110}, and {010} zone axes. Lattice parameters are given in Table 1. The molecular packing in the orange form is shown in Fig.

Table 1. Lattice Parameters for Polymorphs of 5-DMP

	Orange form	Yellow form
<i>a</i> /Å	13.671 (3)	12.27 (3)
<i>b</i> /Å	14.899 (2)	9.44 (2)
<i>c</i> /Å	6.186 (2)	12.42 (3)
$\beta$ /°	97.27 (2)	114.80 (1)
<i>V</i> /Å <sup>3</sup>	1249.9 (5)	1306
<i>Z</i>	4	4
Space group	<i>P2<sub>1</sub>/a</i>	<i>Cc</i>
Reference	12	11

2 as a projection onto the (010) face (for clarity, only half of the molecules in a unit cell are illustrated). The nearest-neighbor molecules are related by a translational symmetry. Since the space group of the orange form is  $P2_1/a$  ( $C_{2h}^5$ ), the exciton wavefunction of the  $B_u$  symmetry is allowed for light polarized parallel with the  $ac$  plane and that of the  $A_u$  symmetry is active along the  $b$  axis.

**The Yellow Form:**<sup>11)</sup> Crystals of the yellow form were transparent laths and elongated along the  $c$  axis. The prominent zone axes were {010} and {110} (Fig. 1(b)).

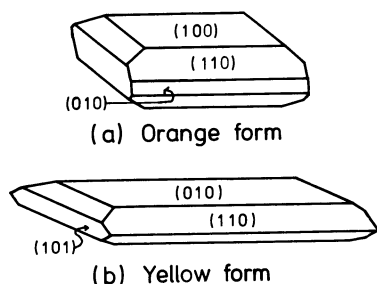


Fig. 1. Crystal morphology for (a) the orange form and (b) the yellow form.

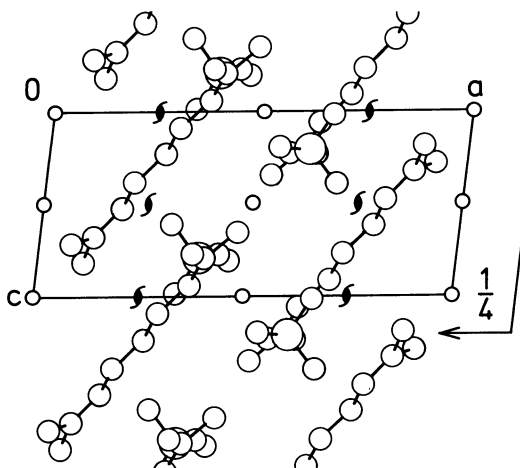


Fig. 2. Crystal structure of the orange form with symmetry symbols.

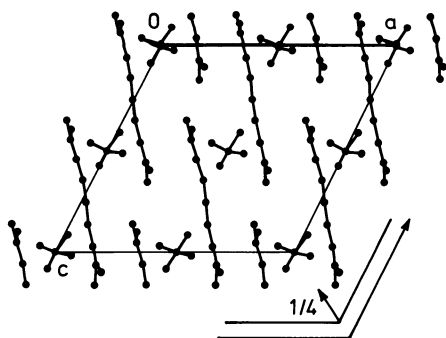


Fig. 3. Crystal structure of the yellow form with symmetry symbols.

Lattice parameters are shown in Table 1. The arrangement of the molecules in a crystal is shown in Fig. 3, where the molecules are stacked along the  $c$  axis. Since the space group of the yellow form is  $Cc$  ( $C_s^4$ ), the exciton wavefunctions which have an  $ac$  component and a  $b$  component have  $A'$  and  $A''$  symmetries, respectively.

**Measurements.** Reflection spectra were measured on a microscopic spectrophotometer as reported previously.<sup>5)</sup> The reflectivities were converted to molar absorption coefficients by a K-K transformation on a FACOM M-382 computer of the Nagoya University Computation Center. The computation program was based on the method of Ahrenkiel.<sup>20)</sup> The absorption spectra of the monomer in solution were measured on a Hitachi 330 spectrophotometer.

## Results

**Solution Spectrum.** The spectrum of a methanol solution at room temperature is shown in Fig. 4. Measurements of aqueous and chloroform solutions gave almost the same results. Although the absorption band has an asymmetric shape, vibrational structures are not clear. The oscillator strength is 1.08, and the transition-dipole length is estimated to be 2.02 Å.

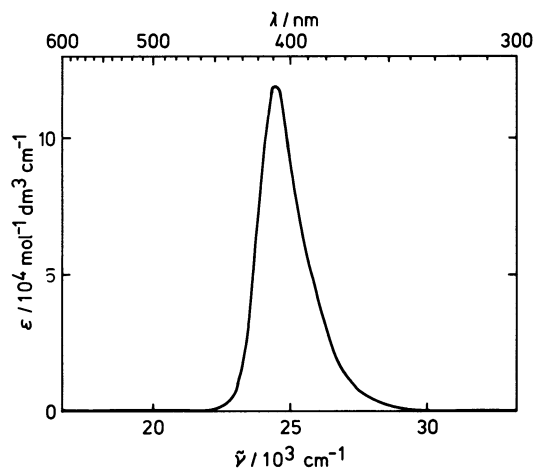


Fig. 4. Solution spectrum of 5-DMP at room temperature in methanol ( $c=2 \times 10^{-5}$  mol dm<sup>-3</sup>).

**Crystalline Reflection Spectra. The Orange Form:** Figure 5 shows the reflection spectra obtained for several polarization directions on the (010) face. Spectra 1 and 3, respectively, are for parallel and perpendicular polarizations to the long axis of a cation molecule. It should be pointed out that a single reflection peak at 21500 cm<sup>-1</sup> is found in the spectrum 3. For the other polarization directions, there are at least two reflection peaks. One of them is apparently due to the  $\pi\pi^*$  transition of the cation molecule, and the other in the 21500 cm<sup>-1</sup> region is clearly due to an extra transition which appears only in a crystal through an intermolecular interaction.

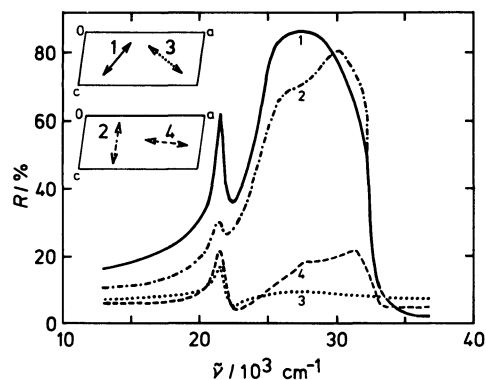


Fig. 5. Reflection spectra from the (010) face of the orange form.

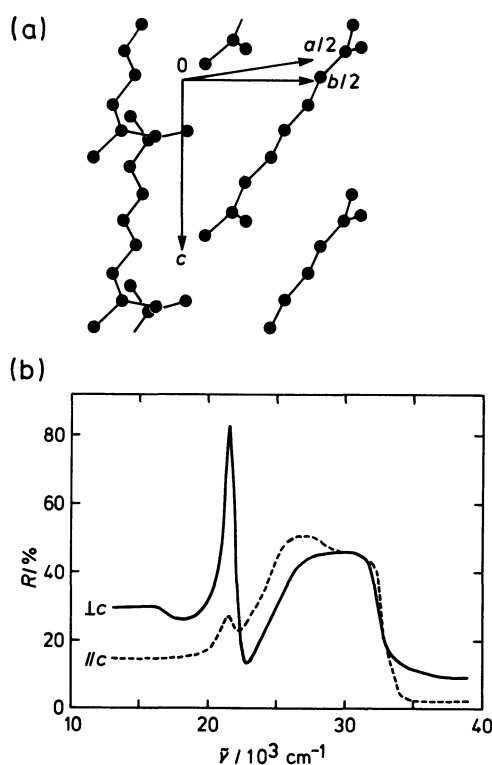


Fig. 6. (a) Projection onto the (110) face of the orange form and (b) the reflection spectra from the (110) face.

The direction of the transition moment for the latter one is distinct from that of the  $\pi\pi^*$  transition.

Figure 6(a) shows a projection onto the (110) face. In this projection, two kinds of molecular orientations are shown, where the direction connecting the nitrogen atoms of the adjacent cation molecules is almost perpendicular to the  $c$  axis. The reflection spectra from the (110) face is shown in Fig. 6(b). On this face, the intensity of the  $21500\text{ cm}^{-1}$  band is maximum for the direction perpendicular to the  $c$  axis, and the  $B_u$  symmetry state of the  $\pi\pi^*$  transition is greatly blue shifted in this direction. The apparent shift may be partly due to an interference effect by the

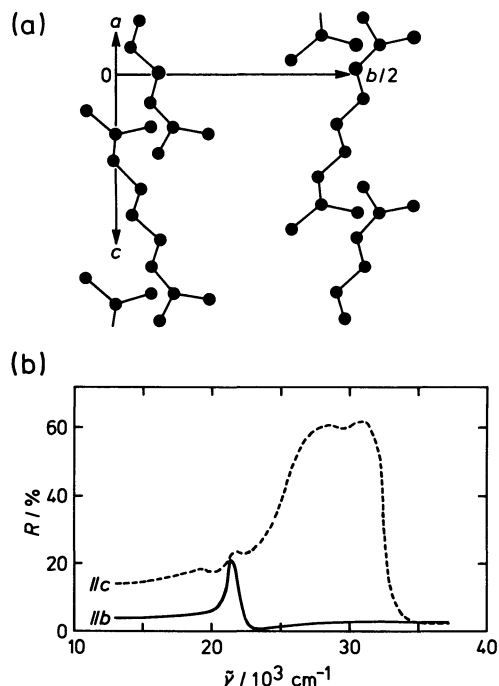


Fig. 7. (a) Projection onto the (100) face of the orange form and (b) the reflection spectra from the (100) face.

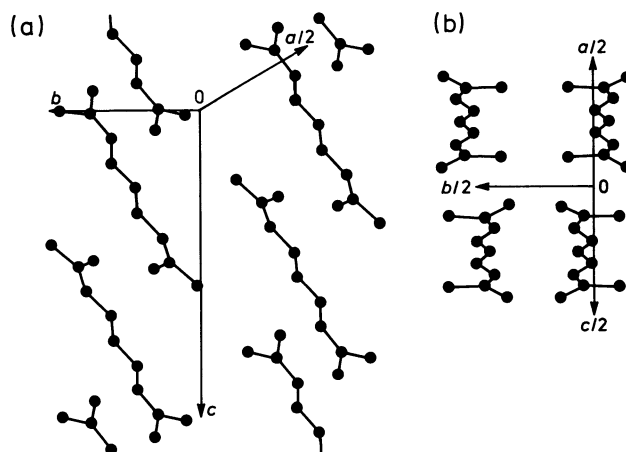


Fig. 8. (a) Projection onto the (110) and (101) faces of the yellow form.

$21500\text{ cm}^{-1}$  transition, since a sharp dip at  $23000\text{ cm}^{-1}$  might influence the reflectance of the  $\pi\pi^*$  transition at the lower edge.

In a projection onto the (100) face (Fig. 7(a)), the  $\text{N}\cdots\text{N}$  direction is almost vertical to the developed face. Figure 7(b) shows the reflection spectra from the (100) face. In the  $c$ -axis spectrum, the  $21500\text{ cm}^{-1}$  peak is observed very weakly and the  $\pi\pi^*$  transition is largely blue shifted. In the  $b$ -axis spectrum, only a single band is found at  $21500\text{ cm}^{-1}$ .

**The Yellow Form:** Figures 8(a) and (b) show projections onto the (110) and (101) faces. Figure 9 shows the reflection spectra from the (010), (110), and

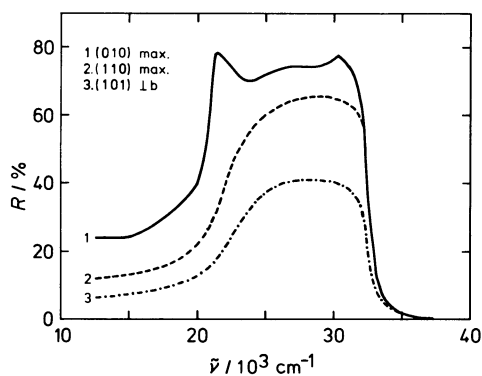


Fig. 9. Reflection spectra from the (010), (110), and (101) faces of the yellow form.

(101) faces. The polarizations of light which gives the maximum reflectivities are almost parallel to the projections of the long axis of the cation molecules. This direction deviates by  $5^\circ$  from the long axis on the (010) face. On each face, the reflectivities with the polarization perpendicular to the maximum direction are less than 5%. Broad reflection bands are attributed mostly to the  $\pi\pi^*$  transition on each face. On the (010) face, a high reflectance for a wide energy range of 1.5 eV ( $\approx 12000\text{ cm}^{-1}$ ) is shown; it exhibits a peak at the lower edge of  $21200\text{ cm}^{-1}$ . This reflection band has been noticed as a typical quasi-metallic reflection band.<sup>13,21,22)</sup>

**K-K Transforms to Absorption Spectra. The Orange Form:** The absorption spectra were obtained by a K-K transformation of the reflection spectra from the (010), (1 $\bar{1}$ 0), and (100) faces (Figs. 10, 11, and 12). A remarkable feature of the absorption spectra is that the  $21500\text{ cm}^{-1}$  peak shows a quite anomalous polarization behavior. As previously mentioned, the direction of the transition moment is different from that of the  $\pi\pi^*$  transition on the (010) face, and the intensity is particularly strong on the (1 $\bar{1}$ 0) face. Considering the dichroic ratio on these crystalline faces, the direction of the transition moment of the  $21500\text{ cm}^{-1}$  band is deduced to be on the line connecting the N...N atoms; therefore, the character of this transition is assigned to the charge-resonance (CR) band between adjacent stacked molecules.

Another conspicuous characteristic of the spectra is that the peak positions of the  $\pi\pi^*$  transition (MX band) are shifted to blue in many directions, presumably because the higher tail of the  $21500\text{ cm}^{-1}$  band interferes with the rise of the reflection spectra due to the  $\pi\pi^*$  transition. In the consideration of the energy levels of the MX band, this effect must be taken into account by assuming that the center of the MX band is blue shifted.

The absorption spectra of the (100) face along the  $c$  axis show weak peaks in the  $21500\text{ cm}^{-1}$  region and a

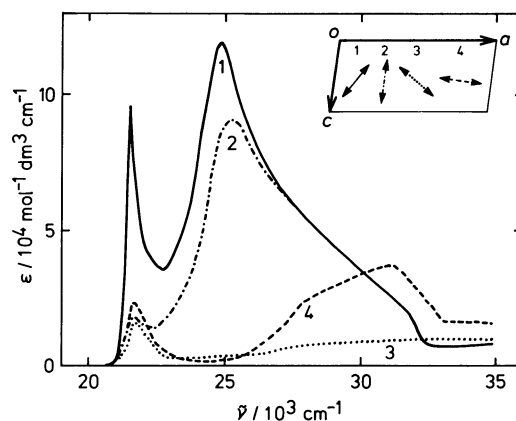


Fig. 10. Absorption spectra for the (010) face of the orange form.

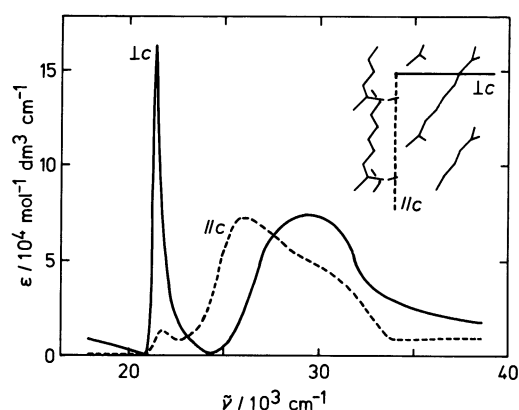


Fig. 11. Absorption spectra for the (1 $\bar{1}$ 0) face of the orange form.

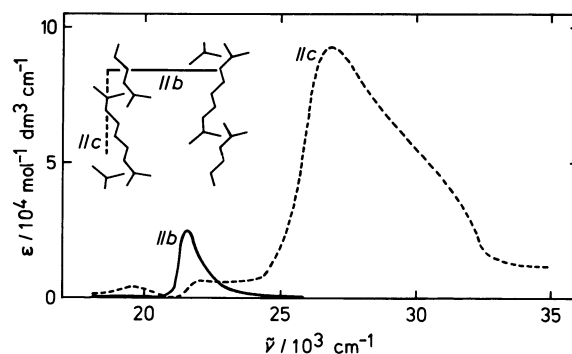


Fig. 12. Absorption spectra for the (100) face of the orange form.

very strong band in the region  $27000\text{--}32000\text{ cm}^{-1}$ . Along the  $b$  axis, the  $\pi\pi^*$  transition shifts to red and overlaps with the CR band at  $21500\text{ cm}^{-1}$ . These tendencies of the band shift and the splitting will be discussed in the next section.

**The Yellow Form:** The transformed absorption

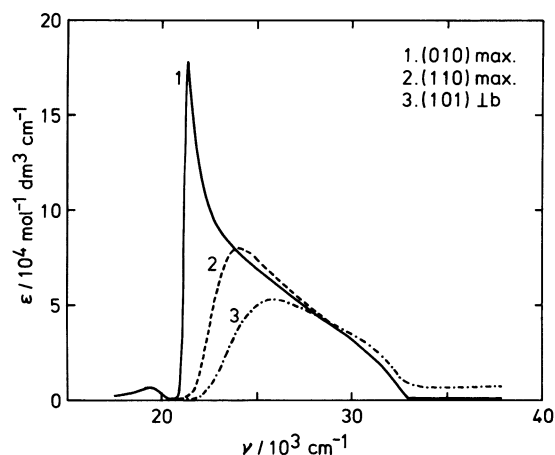


Fig. 13. Absorption spectra for the (010), (110), and (101) faces of the yellow form.

spectra for the yellow form are shown in Fig. 13. A very sharp peak at  $21300\text{ cm}^{-1}$  and a broader peak near the  $23000\text{ cm}^{-1}$  region were obtained on the (010) face. This is a characteristic feature of a strong metallic reflection band. The presence of two peaks was recognized in the earlier work of Fanconi et al.<sup>20</sup> The band feature may be due to the overlapping and mixing of the CR and MX configurations. Such a sharp peak is not found for the other faces, (110) and (101), although weak reflectivity humps are found in the  $21500\text{ cm}^{-1}$  region. In this crystal, the effect of the CR interaction seems to appear only when the energy level of the MX configuration is close to that of the CR configuration.

**Comparison with 3-DMP.** In a previous study regarding the reflection spectra of 3-DMP,<sup>18</sup> we observed only an MX-type excited state; any token of the CR band was not detected. This is reasonable since the intermolecular overlap between cation molecules is not large and no specific interaction exists between nitrogen atoms of the adjacent molecules. In 5-DMP crystals, an additional transition is found which is due to an intermolecular electron exchange interaction due to a significant molecular overlap. The cause of such a contrast may be that 5-DMP has a longer conjugated system than 3-DMP; therefore, both the donor and the acceptor properties are enhanced in 5-DMP and the CR interaction is increased. The length of the conjugated chain in pentamethine may be optimum because a chain that is too long may reduce the charge density of the HOMO and the LUMO at the terminal nitrogen atoms.

### Discussion

A criterion of the J band is a sharp and red-shifted

absorption band, a characteristic of the aggregate; then, the  $21500\text{ cm}^{-1}$  band of the orange form is a typical J band. Although the condition for the appearance of a J band is not yet clear, the present experimental result may provide a key for resolving this long-standing problem.

The  $21500\text{ cm}^{-1}$  band is ascribed to a transition which is different from the  $\pi\pi^*$  transition because the reflection spectra from the (010) face of the orange form (Fig. 5) show two strong peaks in the  $21500\text{ cm}^{-1}$  and  $27000\text{ cm}^{-1}$  regions. These are difficult to explain by an exciton-type band splitting of a single  $\pi\pi^*$  transition. In the spectra on the (010) face, only the  $B_u$  state is observable using normally incident light. Also, a single transition should produce a single peak. Such a theoretical prediction has been confirmed from many experiments on various crystals. The direction of the transition moment of the  $21500\text{ cm}^{-1}$  band should be determined from polarization measurements for all possible faces. However, the actual spectra are rather complicated because of the intensity borrowing or the mixing with the  $\pi\pi^*$  transition.

In our previous studies on the spectra of cyanine dye crystals,<sup>4,5</sup> we have shown that the charge-resonance (CR) type band is strongly mixed with the molecular-exciton (MX) type band. Although the polarization of the charge-transfer (CT) band of the electron donor-acceptor complex is believed to lie along the direction connecting the centers of the HOMO of the donor and the LUMO of the acceptor molecules, the present CR band gives a different result. It shows that the transition moment is directed along the line connecting the N...N atoms of the adjacent dye molecules. This means that the nitrogen atoms of the cyanine dye may take on a canonical polar structure at the moment of a transition in which CR takes place between the N...N<sup>+</sup> atoms. This argument is based on the fact that the intensity of the CR band arises from two sources; one is a genuine CR transition moment directed along the N...N direction, and the other comes from a mixing with the MX configuration.

By this assignment, the characteristic sharp band shape of the J band can be ascribed to the nitrogen  $\pi$  orbital since a sharp band feature is often found in the photoelectron spectra of the nonbonding orbital.<sup>23</sup> A sharp band shape is considered as an evidence of a small coupling with a molecular vibration; in other words, a nonbonding character of the nitrogen  $\pi$  orbital may give a small coupling with a molecular vibration in the CR spectra.

The present dye in solution exhibited a broad single absorption (Fig. 4). However, Gerhold observed two overlapping peaks in low temperature glass and estimated the vibrational interval at  $1150\text{ cm}^{-1}$ .<sup>14</sup> The blue-shifted  $\pi\pi^*$  bands are much

broader in the crystalline spectra than in the solution, but the 21500 cm<sup>-1</sup> band is sharp without any vibrational progression.

**Theoretical Consideration on the Electronic States in the Crystals.** In order to discuss the interaction of the CR configuration with the MX configuration in the crystal, the effect of the intermolecular overlap interaction is considered here in detail. As previously mentioned, the interactions of the nearest-neighbor molecules extend along the *c* axis for both orange and yellow crystals. Therefore, we can restrict our treatment to a one-dimensional array of the molecules along the *c* axis.

An intense electronic absorption is found for the electronic transition between the HOMO ( $\varphi$ ) and the LUMO ( $\theta$ ), and a charge transfer also occurs between the HOMO and the neighbor's LUMO. From the previous discussion regarding the direction of the CR band, an interaction between nitrogen atoms may be more important. However, in the following argument we consider interactions between molecular orbitals. The ground configuration of the system is given by

$$\Phi_G = |\cdots \varphi_{i-1} \bar{\varphi}_{i-1} \varphi_i \bar{\varphi}_i \varphi_{i+1} \bar{\varphi}_{i+1} \cdots|, \quad (1)$$

and the CR configuration is described by

$$\Phi_{CR}^\pm = \frac{1}{\sqrt{2N}} \sum_{i=1}^N (\Phi_{i \rightarrow i+1} \pm \Phi_{i+1 \rightarrow i}), \quad (2)$$

where

$$\begin{aligned} \Phi_{i \rightarrow i+1} = & \frac{1}{\sqrt{2}} (|\cdots \varphi_{i-1} \bar{\varphi}_{i-1} \theta_{i+1} \bar{\varphi}_i \varphi_{i+1} \bar{\varphi}_{i+1} \cdots| \\ & + |\cdots \varphi_{i-1} \bar{\varphi}_{i-1} \varphi_i \bar{\theta}_{i+1} \varphi_{i+1} \bar{\varphi}_{i+1} \cdots|) \end{aligned} \quad (3a)$$

and

$$\begin{aligned} \Phi_{i+1 \rightarrow i} = & \frac{1}{\sqrt{2}} (|\cdots \varphi_{i-1} \bar{\varphi}_{i-1} \varphi_i \bar{\theta}_i \varphi_{i+1} \bar{\varphi}_{i+1} \cdots| \\ & + |\cdots \varphi_{i-1} \bar{\varphi}_{i-1} \varphi_i \bar{\varphi}_i \varphi_{i+1} \bar{\theta}_i \cdots|). \end{aligned} \quad (3b)$$

The MX configuration can be represented for the translationally equivalent molecules by

$$\Phi_{MX} = \frac{1}{\sqrt{N}} \sum_{i=1}^N \Phi_i \quad (4)$$

where

$$\begin{aligned} \Phi_i = & \frac{1}{\sqrt{2}} (|\cdots \varphi_{i-1} \bar{\varphi}_{i-1} \bar{\varphi}_i \varphi_{i+1} \bar{\varphi}_{i+1} \cdots| \\ & + |\cdots \varphi_{i-1} \bar{\varphi}_{i-1} \varphi_i \bar{\theta}_i \varphi_{i+1} \bar{\varphi}_{i+1} \cdots|). \end{aligned} \quad (5)$$

Now let us consider the matrix elements between

these configurations by calculating the transfer integrals which are approximated as being proportional to the overlap integrals between the relevant molecular orbitals. The abbreviated formulae for the overlap integrals are given by

$$\begin{aligned} S_{11} &= \langle \varphi_i | \varphi_{i+1} \rangle, & S_{12} &= \langle \varphi_i | \theta_{i+1} \rangle, \\ S_{21} &= \langle \theta_i | \varphi_{i+1} \rangle, & S_{22} &= \langle \theta_i | \theta_{i+1} \rangle. \end{aligned} \quad (6)$$

An approximate formula for estimating the transfer integral is given by

$$t_{mn} = k S_{mn} \quad (m, n=1, 2). \quad (7)$$

The symmetries of the  $\varphi$  and  $\theta$  orbitals in this system give a relation  $S_{12} = -S_{21}$ ; hence, the matrix element between the  $\Phi_G$  and the  $\Phi_{CR}^-$  configurations is given by

$$\begin{aligned} \langle \Phi_G | \mathcal{H} | \Phi_{CR}^- \rangle &= \frac{1}{\sqrt{N}} \sum_{i=1}^N (\langle \varphi_i | \mathcal{H} | \theta_{i+1} \rangle - \langle \theta_i | \mathcal{H} | \varphi_{i+1} \rangle) \\ &= \sqrt{N} k (S_{12} - S_{21}) = 2\sqrt{N} k S_{12}. \end{aligned} \quad (8)$$

The  $\Phi_{CR}^+$  configuration interacts with the  $\Phi_{MX}$  configuration and the matrix element is calculated as

$$\begin{aligned} \langle \Phi_{CR}^+ | \mathcal{H} | \Phi_{MX} \rangle &= \frac{1}{\sqrt{2}} \cdot \frac{1}{N} \sum_{i=1}^N (\langle \Phi_{i \rightarrow i+1} | \mathcal{H} | \Phi_i \rangle \\ &+ \langle \Phi_{i-1 \rightarrow i} | \mathcal{H} | \Phi_i \rangle + \langle \Phi_{i+1 \rightarrow i} | \mathcal{H} | \Phi_i \rangle \\ &+ \langle \Phi_{i \rightarrow i-1} | \mathcal{H} | \Phi_i \rangle) \\ &= \sqrt{2} k (S_{22} - S_{11}). \end{aligned} \quad (9)$$

The matrix element given in Eq. 8 is renormalized to evaluate the contribution of the  $\Phi_{CR}^-$  configuration to the ground state per molecule. Then, the secular equation (including the  $\Phi_G$  and the  $\Phi_{CR}^-$  configurations) is given by

$$\begin{vmatrix} -E & 2kS_{12} \\ 2kS_{12} & E_{CR} - E \end{vmatrix} = 0. \quad (10)$$

The mixing of the  $\Phi_{MX}$  and the  $\Phi_{CR}^+$  configurations is calculated by solving the secular equation

$$\begin{vmatrix} E_{CR} - E & \sqrt{2} k (S_{22} - S_{11}) \\ \sqrt{2} k (S_{22} - S_{11}) & E_{MX} - E \end{vmatrix} = 0. \quad (11)$$

The calculation of the overlap integrals is performed by a previously reported method,<sup>24)</sup> and obtained values are as shown in Table 2. The magnitudes of these integrals are fairly large for an intermolecular interaction and the transfer integrals are estimated by setting  $k = -15$  eV in Eq. 7. This choice of  $k$  is reasonable in view of the Mulliken-

Table 2. Molecular Integrals between the MO's of Stacked Dye Molecules

Crystalline form	MO	$S_{mn}$		$\langle \Phi_G   \mathcal{H}   \Phi_{CR}^- \rangle$ eV	$\langle \Phi_{CR}^+   \mathcal{H}   \Phi_{MX} \rangle$ eV
		$\varphi_{i+1}$	$\theta_{i+1}$		
Orange	$\varphi_i$	0.00965	0.00872	-0.3105	0.3837
	$\theta_i$	-0.01198	-0.00844		
Yellow	$\varphi_i$	0.00232	0.00477	-0.1362	0.1421
	$\theta_i$	-0.00431	-0.00438		

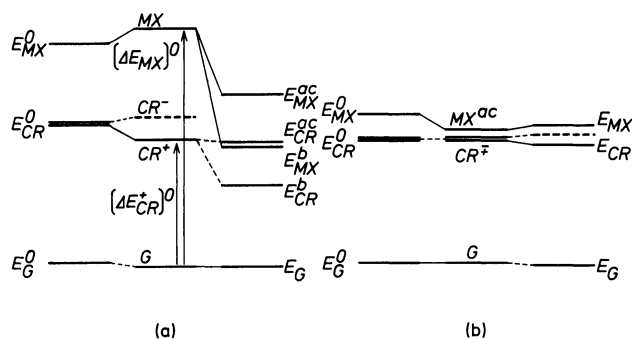


Fig. 14. Calculation procedures of the electronic states in the crystals; (a) for the orange form and (b) for the yellow form.

Wolfsberg-Helmholtz formula. It states that  $k=KW$ , since if we take the orbital energy of HOMO at  $W=-10$  eV then  $K=1.5$ .<sup>24)</sup>

**The Orange Form:** The calculation procedure is shown in Fig. 14(a), where the interaction of the  $\Phi_{CR}^+$  and the  $\Phi_{MX}$  configurations is first considered; then, the exciton band splittings in the  $CR^+$  and the  $MX$  states are evaluated.

The initial diagonal energies for the orange form are set at  $E_{CR}^0=22800$  cm<sup>-1</sup> and  $E_{MX}^0=29300$  cm<sup>-1</sup>, respectively. The blue shift of the  $MX$  state, compared to a solution spectra, is assumed to harmonize the calculated energy levels with the observed spectra. The transfer integrals of the orange form are apparently larger than those of the yellow form (Table 2). Accordingly, the mixing of the  $\Phi_{CR}^+$  configuration with the  $\Phi_{MX}$  configuration is more important in the orange form than in the yellow form. After solving the secular equations, 10 and 11, the energy levels of the  $CR^+$  and the  $MX$  states were found at  $(\Delta E_{CR}^+)^0=21900$  cm<sup>-1</sup> and  $(\Delta E_{EX})^0=30800$  cm<sup>-1</sup>, respectively, where the stabilization of the ground state was taken into account. These energy levels correspond to the center of the Davydov components. The transition moments were obtained as being a vector sum of the  $CR^-$  and the  $MX$ -type moments multiplied by coefficients which were obtained by solving the secular equations. In this treatment, the  $CR$ -type moment was taken as the vector connecting the two nitrogen atoms of adjacent dye molecules.

The transition length of the  $MX$ -type moment was set at 2.2 Å, larger by 10% than the solution's value. Such a bathochromism of the  $MX$  transition might exist due to the effect of the  $CR$  interaction.

In order to explain the splitting of the crystalline  $MX$  states, the exciton energy shifts were calculated for the measured faces by a dipole-dipole approximation.<sup>5)</sup> The dipole sum was extended for molecules in a disc with a radius of 200 Å and a depth of 20 Å, placed in the crystalline surface. The wavefunctions for a  $MX$  state having  $A_u$  and  $B_u$  symmetries are given by

$$A_u : \Psi_b = \frac{1}{\sqrt{N}} \sum_{i=1}^N (\Psi_{1i} - \Psi_{2i} + \Psi_{3i} - \Psi_{4i}) e^{i\mathbf{k} \cdot \mathbf{R}_i} \quad (12a)$$

and

$$B_u : \Psi_{ac} = \frac{1}{\sqrt{N}} \sum_{i=1}^N (\Psi_{1i} - \Psi_{2i} - \Psi_{3i} + \Psi_{4i}) e^{i\mathbf{k} \cdot \mathbf{R}_i} \quad (12b)$$

where  $i$  is the numbering of the unit cell, and 1, 2, 3, and 4 designate the molecular sites.  $\Psi_{1i}$  means that the original site of the  $i$ -th cell is excited and others are in the ground state.  $\Psi_{2i}$ ,  $\Psi_{3i}$ , and  $\Psi_{4i}$  are wavefunctions in which excitation occurs at sites related to the original site by the space group operators: center of symmetry, screw axis and glide plane, respectively.

The results of the calculation for the energy levels and intensities are shown in Table 3. Agreement between the observed and the calculated results is quite reasonable in spite of the complicated patterns of the spectra for the respective faces.

On the (010) face, only the  $B_u$  component is expected to appear and the observed band positions and intensities are well explained by the mixing of the  $\Phi_{CR}^+$  configuration with the  $\Phi_{MX}$  configuration. The  $MX$  band for the  $\perp c$  polarization was found at 28000–31000 cm<sup>-1</sup> region, and such an unusual blue shift might be appeared by a decrease of the reflectivity at 26000 cm<sup>-1</sup> region which is caused by the interference effect of the dip at 22500 cm<sup>-1</sup>.

With the (110) face, the calculated spectrum for the  $\parallel c$  direction is in good agreement with the observed spectrum. However the  $\perp c$  component shows two discrepancies. First, the band intensity at the 21500 cm<sup>-1</sup> region is much smaller than the observed

Table 3. Polarized Crystalline Spectra of the Orange Form

Face	pol. axis	CR				MX			
		$\Delta E_{\text{CR}}^{\text{a)}}$ /10 <sup>3</sup> cm <sup>-1</sup>		$f$		$\Delta E_{\text{MX}}^{\text{a)}}$ /10 <sup>3</sup> cm <sup>-1</sup>		$f$	
		Obsd	Calcd	Obsd	Calcd	Obsd	Calcd	Obsd	Calcd
(010)	$\parallel c$	21.6	21.1	0.12	0.28	25.2	24.2	2.90	2.81
	$\perp c$	21.6		0.21	0.43	31.0		1.30	0.78
	$\parallel L^{\text{b)}$	21.5		1.30	0.65	24.8		3.15	3.55
	$\perp L^{\text{b)}$	21.7		0.13	0.06	—		—	0.04
(1 $\bar{1}$ 0)	$\parallel c$	21.7	21.8	0.21	0.28	26.0	25.4	3.30	2.81
	$\perp c$	21.4	21.8, 19.8	1.47	0.20, 0.07	29.0	25.4, 21.6	4.32	0.53, 0.14
(100)	$\parallel c$	22.0	23.5	0.12	0.28	26.8	28.0	3.52	2.81
	$\parallel b$	—	20.2	—	0.14	21.5	22.2	0.19	0.26

a)  $\Delta E_{\text{CR}} = E_{\text{CR}} - E_{\text{G}}$  and  $\Delta E_{\text{MX}} = E_{\text{MX}} - E_{\text{G}}$ . b) Parallel and perpendicular to the molecular long axis.

Table 4. Polarized Crystalline Spectra of the Yellow Form

Face pol. axis		CR				MX						
		$\Delta E_{\text{CR}}^{\text{a)}}$ /10 <sup>3</sup> cm <sup>-1</sup>		$f$		$E_{\text{MX}}^{\text{a,c,b)}$	$\Delta E_{\text{MX}}^{\text{a)}}$ /10 <sup>3</sup> cm <sup>-1</sup>		$f$			
		Obsd	Calcd	Obsd	Calcd		Obsd	Calcd	Obsd	Calcd		
						10 <sup>3</sup> cm <sup>-1</sup>						
(010)	max. min.	24.6 —	}	22.2	1.10 —	1.26 0.00	21.7	21.3 —	}	21.4	4.09 —	2.24 0.05
(110)	max. min.	— —		}	21.7	—	0.75 0.00	22.4		23.8 —	}	22.6
(101)	$\perp b$ $\parallel b$	— —	}		21.9	—	0.04 0.00	26.1	25.7 —	}		26.2

a)  $\Delta E_{\text{CR}} = E_{\text{CR}} - E_{\text{G}}$  and  $\Delta E_{\text{MX}} = E_{\text{MX}} - E_{\text{G}}$ . b) The A' level of the  $\Phi_{\text{MX}}$  configuration.

value in spite of the fact that the CR<sup>+</sup>- and the MX-A<sub>u</sub> states were calculated to be in this region. The sum of these intensities were not sufficient to account for the prominent strong peak. Secondly, the MX level for the  $\perp c$  direction was calculated at 25400 cm<sup>-1</sup> while the observed value was 29000 cm<sup>-1</sup>. This blue shift may have occurred due to an interference of the sharp peak at 21500 cm<sup>-1</sup>.

On the (100) face, the spectrum for the  $b$ -axis polarization gives a single peak and the calculated energies for the CR and the MX states are close together in agreement with the experiment. The peak position for the  $c$  axis is well explained by the calculation. However, the calculated intensity for the 21500 cm<sup>-1</sup> band is larger than the observed one. This may depend on the calculation method.

An alternative approach to the calculation of the energy level is that the splitting of the  $\Phi_{\text{MX}}$  level is first calculated for each face; then, the interaction with the  $\Phi_{\text{CR}}^+$  configuration is considered on each face (Fig. 14(b)). By this method, the mixing coefficient is varied on each face and an overly enhanced intensity for the CR band of the (100) face may be reduced.

**The Yellow Form:** The calculation of the yellow form follows the latter method, and the shift of the  $\Phi_{\text{MX}}$  configuration is evaluated at first by taking  $E_{\text{MX}}^0$

at 23800 cm<sup>-1</sup> with the transition dipole length of 2.2 Å. The dye molecule in the yellow form lies along its long axis perfectly perpendicular to the  $b$  axis; therefore, the A'' component is not expected. In fact, the observed spectra did not show any intensity of the A'' component.

Following the present calculation, the A' level of the  $\Phi_{\text{MX}}$  configuration was calculated at 21700 cm<sup>-1</sup> for the (010) face; it was very close to the assumed CR level,  $E_{\text{CR}}^0 = 21900$  cm<sup>-1</sup>. The coupling between these two configurations is very significant; therefore, the resultant states are regarded as completely mixed states of the  $\Phi_{\text{MX}}$  and  $\Phi_{\text{CR}}^+$  configurations. The observed intensity is much larger than the calculated one. This may be due to the effect of the CR interaction. The sharp pattern of the 21300 cm<sup>-1</sup> band may be regarded as an example of the J band; this is reasonable because it has about 50% of the CR characteristics. However, it should also be mentioned that a metallic reflection band always gives a sharp peak at the lower edge.

On the (110) face, the MX band is predicted to be slightly red shifted, and the observed peak is so shifted. The calculated CR band was not found, presumably because it was buried under the tail of the strong peak situated at the higher-energy side.

The MX band for the (101) face is calculated to



shift to blue; this is in agreement with the observed tendency. The CR band is predicted to be very weak because of a small mixing with the  $\Phi_{MX}$  configuration. No reflection peak was detected at the lower-energy side.

**Concluding Remarks.** The spectral features of the excited states of the orange and the yellow forms of 5-DMP crystals are well explained by a consideration of the CR excited configuration in the  $22000\text{ cm}^{-1}$  region. The transition moment of this transition is directed along the N...N atoms of the adjacent dye molecules, suggesting that the CR occurs between molecules represented by a canonical structure of  $\text{Me}_2\text{N}-\text{C}=\text{C}-\text{C}=\text{C}-\text{N}^+\text{Me}_2$ . A large contribution of this structure to the molecular structure of the orange form is geometrically supported by a precise X-ray analysis.<sup>12)</sup> The sharp envelope of the CR band may be associated with the mechanism of the appearance of the J band; a charge-transfer excitation in the nonbonding orbital of a nitrogen atom occurs in a rigid molecule. Although the J band has been considered to appear due to a red shift of the molecular  $\pi\pi^*$  transition in the aggregates of laterally stacked dyes, the present analysis shows that the genuine origin of the J band is the existence of a new kind of excited configuration which appears in the N...N atoms at a short distance with a favorable molecular overlap in the stacking. A single and strong J-type band may appear when the CR configuration coexists and mixes with the MX configuration of a large transition moment in the same energy region. A separate and sharp J band is found when the CR configuration is situated away from the MX configuration. The spectrum of the (010) face of the yellow form corresponds to the former case, while the spectra of the orange form represent the latter situation. Thus, the spectral features of the aggregates and crystals of cyanine dye are characterized by a CR interaction between the moieties including the nitrogen atoms of the conjugated system of the cyanine dye; the interaction occurs in a specifically favorable molecular stacking. The appearance of the J band is thus explained to be a result of a peculiar intermolecular interaction between the cyanine dye molecules.

This research was supported by a grant in aid of the special research project on the properties of molecu-

lar assemblies (No. 60104002) from the Ministry of Education, Science and Culture.

## References

- 1) H. Kobischke and S. Dähne, *Photogr. Sci. Eng.*, **16**, 173 (1972).
- 2) A. H. Herz, *Photogr. Sci. Eng.*, **18**, 323 (1974).
- 3) S. Dähne, *Photogr. Sci. Eng.*, **23**, 219 (1979).
- 4) J. Tanaka, M. Tanaka, and N. Kanamaru, "Relaxation of Elementary Excitations," ed by R. Kubo and E. Hanamura, Springer-Verlag Berlin Heidelberg (1980), Part IV, pp. 181–194.
- 5) J. Tanaka, M. Tanaka, and M. Hayakawa, *Bull. Chem. Soc. Jpn.*, **53**, 3109 (1980).
- 6) S. Makio, N. Kanamaru, and J. Tanaka, *Bull. Chem. Soc. Jpn.*, **53**, 3120 (1980).
- 7) S. C. Abbi and D. M. Hanson, *J. Chem. Phys.*, **60**, 319 (1974).
- 8) J. Tanaka and M. Shibata, *Bull. Chem. Soc. Jpn.*, **41**, 34 (1968).
- 9) L. Sebastian, G. Weiser, G. Peter, and H. Bässler, *Chem. Phys.*, **75**, 103 (1983).
- 10) L. Sebastian, G. Weiser, and H. Bässler, *Chem. Phys.*, **61**, 125 (1981).
- 11) J. O. Selzer and B. W. Matthews, *J. Phys. Chem.*, **80**, 631 (1976).
- 12) M. Honda, C. Katayama, and J. Tanaka, *Acta Crystallogr., Sect. B.*, to be published.
- 13) B. G. Anex and W. T. Simpson, *Rev. Mod. Phys.*, **32**, 466 (1960).
- 14) M. R. Philpott, *J. Chem. Phys.*, **54**, 2120 (1971).
- 15) P. R. Rimbey, *J. Chem. Phys.*, **67**, 698 (1977).
- 16) S. Dähne, B. Bornowski, B. Grimm, S. Kulpe, D. Leupold, and M. Näther, *J. Signal AM5*, 277 (1977).
- 17) K. Sieber, L. Kutschabsky, and S. Kulpe, *Kristall und Technik*, **9**, 1111 (1974).
- 18) M. Otsu and J. Tanaka, *Bull. Chem. Soc. Jpn.*, **58**, 2468 (1985).
- 19) S. S. Malhotra and M. C. Whiting, *J. Chem. Soc. (London)*, **1960**, 3812.
- 20) R. K. Ahrenkiel, *J. Opt. Soc. Am.*, **61**, 1651 (1971).
- 21) B. M. Fanconi, G. A. Gerhold, and W. T. Simpson, *Mol. Cryst. Liq. Cryst.*, **6**, 41 (1969).
- 22) J. Merski and C. J. Eckhardt, *J. Chem. Phys.*, **75**, 3731 (1981).
- 23) K. Kimura, S. Katsumata, Y. Achiba, T. Yamazaki, and S. Iwata, "Handbook of HeI Photoelectron Spectra of Fundamental Organic Molecules," Japan Scientific Societies Press, Tokyo (1981).
- 24) J. Tanaka and C. Tanaka, *Mol. Cryst. Liq. Cryst.*, **126**, 121 (1985).